



Coastal discharge extremes and their environmental impact on the Sea of Marmara

NÜVİT BERKAY BAŞDURAK

Coastal discharge extremes and their environmental impact on the Sea of Marmara

Nüvit Berkay BAŞDURAK^{*} 

Department of Physical Oceanography, Institute of Marine Sciences, Middle East Technical University, Mersin, Türkiye

Received: 28.08.2023 • Accepted/Published Online: 17.12.2023 • Final Version: 19.03.2024

Abstract: Increases in evaporation driven by global warming change the hydrological cycle by fueling extreme precipitation and exacerbating the frequency and intensity of extreme floods. Combined with the increase in terrestrial waste and pollutants, the changing climate exposes coastal zones to natural hazards. The Sea of Marmara, as an inland sea with a dense coastal population, is more vulnerable to such changes and subject to eutrophication and extreme environmental events (e.g., mucilage). Therefore, quantification of daily and along-coast variation of river discharge and evaluation of its annual trend of extremes are crucial. The daily discharges from the coastal watersheds Biga, Gönen, Susurluk, İznik-Gölayağı, and İzmit-Kiraz during the period 2010–2020 were evaluated using the observed stream flows at the gages near the coast. The extreme daily discharges observed in each watershed are 350, 250, 600, 18, and 45 m³ s⁻¹, respectively. The upper limits for coastal discharges during flood events were estimated as 175, 100, and 300 m³ s⁻¹ for the first three watersheds. Daily discharge extremes exhibit seasonal and spatial variations along the coastline, with higher flow rates predominantly occurring in the winter and early spring. The onsets of these variations differ, particularly among the southern rivers, and this spatial-temporal change is examined in relation to net precipitation rates and geomorphological characteristics.

Key words: The Sea of Marmara, coastal discharge, daily runoff extremes, pollution, river basins

1. Introduction

The interactions among oceanographic, hydrological, and atmospheric processes result in floods in coastal areas that are particularly vulnerable to climate change. River deltas, beaches, estuaries, and lagoons are considered particularly vulnerable to the adverse effects of climate change, such as warming sea waters and increasing sea levels that disrupt marine and coastal ecosystems (Elliott et al., 2019). In addition to these stresses, the intense urbanization of coastal margins and human activities related to industrial and agricultural deteriorate the coastal and marine environment (i.e. industrial, agricultural, and urban waste and pollutants) (He and Silliman, 2019). Increasing concentrations of waste and pollutants draining into the coastal and riverine waters, coupled with extreme precipitation events, pose a greater threat to the ecosystem's health. The Sea of Marmara is experiencing these cumulative stresses (Yücel et al., 2021), e.g., increasing sea surface temperature and salinity trends (Latif et al., 2022). As it is an intercontinental inland sea, the consequences of the changes in the hydrochemical and biological characteristics of the ecosystem affect the interconnecting seas, namely the Black and Aegean Seas (Tuğrul et al., 2002).

Estuarine dynamics control the general circulation of the Sea of Marmara, with the deeper Mediterranean waters, characterized by higher salinity, and the brackish surface waters from the Black Sea entering through the Çanakkale and İstanbul straits and setting a two-layer flow structure (Ünlüata et al., 1990; Beşiktepe et al., 1994). The two-layer ecosystem of the Sea of Marmara has been drastically modified by the nutrient and pollutant inputs from the Black Sea, as well as by domestic and industrial discharges from the Marmara watersheds. This has led to the development of eutrophication conditions and a shifting of the depth of nutricline and oxycline upward over the last three decades (Tuğrul et al., 2015; Ediger et al., 2016). The sea snout (mucilage) formations observed in the Sea of Marmara in 2021 signal a declining resilience of the ecosystem under multiple stressors (Savun Hekimoğlu and Gazioğlu, 2021) and are potentially linked to changing nutrient input from the watersheds. Determining the daily coastal discharge from the rivers is crucial because (i) when combined with high nutrient concentrations, it has the potential to trigger extreme events (e.g., sea snout); and (ii) it plays a key role in the deoxygenation of the sea. However, studies on the Sea of Marmara rivers are limited, either focusing on major rivers for specific years (Algan,

* Correspondence: berkay@ims.metu.edu.tr

2006) or providing a general analysis of stream flows at larger time scales (Yildiz et al., 2018). A recent study has indicated that coastal discharges from the northern (Trakya), eastern, and southern basins are 3%, 17%, and 80% of the total discharge, respectively, with variations ranging between 1.5 and 15 km³ per year over the last decade (Başdurak, 2023).

Building on this identified knowledge gap, the aims of this study are to evaluate the daily coastal discharges from the coastal watersheds of the Sea of Marmara for the last decade, to explore the extreme events in relation to precipitation and evaporation, and to discuss their potential impact on the marine environment. To achieve these aims, daily streamflow observation tables from the General Directorate of State Hydraulic Works (¹DSI, 2021) are used for the Biga, Gönen, Susurluk, İznik-Gölayağı, and İzmit-Kiraz watersheds; the former three have the biggest surface area in the region with agricultural land use, and the latter two drain into the gulfs characterized by

urban and industrial land use. These watersheds primarily influence the Sea of Marmara, apart from the fluxes through the straits, due to their relatively high coastal flow rates (Başdurak, 2023), the anthropogenic activities, and nutrient loads associated with these basins (Ozbayram et al., 2022; Tavsanoğlu and Akbulut, 2019).

2. Materials and methods

2.1. Study area

The surface area of the coastal watershed of the Sea of Marmara is 42,218 km², characterized by narrow and steep northern regions and shallow and wide southern regions (Figure 1). The İstanbul and Çanakkale straits diagonally separate the coastal watershed into two parts, i.e. the European and Asian basins in Thrace and Anatolia, respectively, with surface areas of 4330 km² and 37,390 km². The study area comprises two eastern basins and three southern basins (Figure 1, inset), with an average elevation of 500 m and a peak altitude of 2540 m (Uludağ

¹Devlet Su İşleri (2021). Akım gözlem yıllıkları (in Turkish) [online]. Website: <https://www.dsi.gov.tr/> [accessed 2021/09/22]

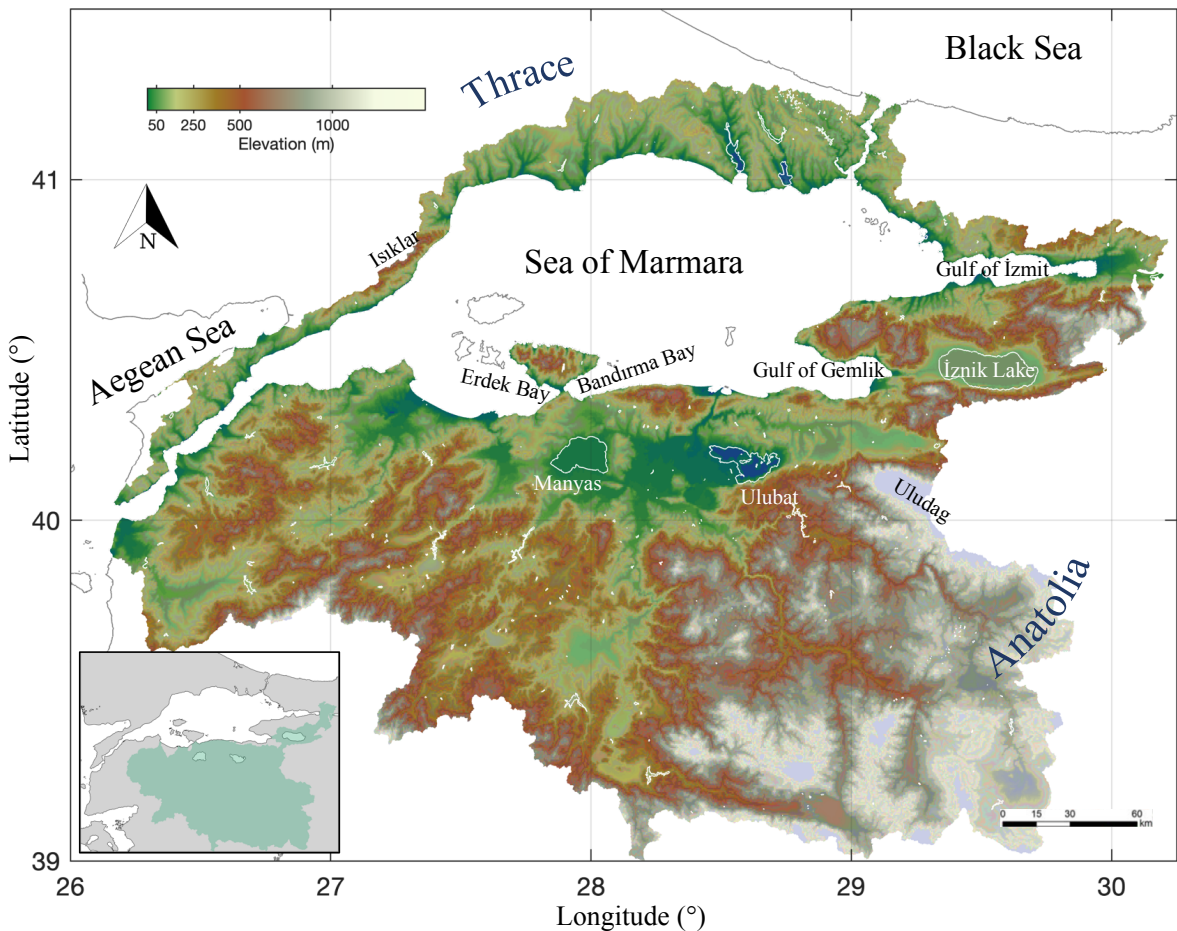


Figure 1. Topographic map of the watershed of the Sea of Marmara; white lines show the boundaries of the terrestrial water bodies. The inset shows the study area.

Mountain). These basins include three lakes: Manyas, Ulubat, and İznik, which feed the stream network near the coast, with the former two located in the southern basin.

The study area was chosen based on the size of the watersheds and the vulnerability of the nearby coastal zone. The southern watersheds are Biga, Gönen, and Susurluk, with surface areas of 2112 km², 2090 km², and 22,900 km², respectively; the former two drain into the Erdek Bay, while the latter drains into the Bandırma Bay (Figure 2). The Susurluk Basin is the biggest watershed in the region, contributing agricultural input to the coast. Runoff from the eastern watersheds, namely Gölayağı and Kiraz, drains into the gulfs of İzmit and İznik, carrying most of the industrial and urban load to the coast.

The geological features of the watersheds are diverse, primarily comprising sedimentary, metamorphic, and volcanic rocks near the coast (Figure A). Thus, hydraulic conductivity varies significantly along the stream network,

which affects the downstream impact of flood intensity during heavy rainfall events. Alluvial and fluvial deposits exist at the river mouths and around the lakes. In the Susurluk Basin, metamorphic rocks (less permeable) separate the alluvial wetland at the river mouth from the sedimentary rocks surrounding the Manyas and Ulubat lakes.

2.2. Daily streamflow

The European Digital Elevation Model (EUDEM v.1.1) and the European River Network (EU-HYDRO v.1.3) were used to extract the watershed boundaries and stream network at a 25-m horizontal resolution (Figure 2). Annual streamflow observation tables of the General Directorate of State Hydraulic Works (DSI) were used to determine the daily change in coastal river discharges (red full circles, Figures 2 and 3a). Firstly, the points along the stream tributaries closest to the stations were identified (depicted as black markers in Figures 2 and 3a). Secondly,

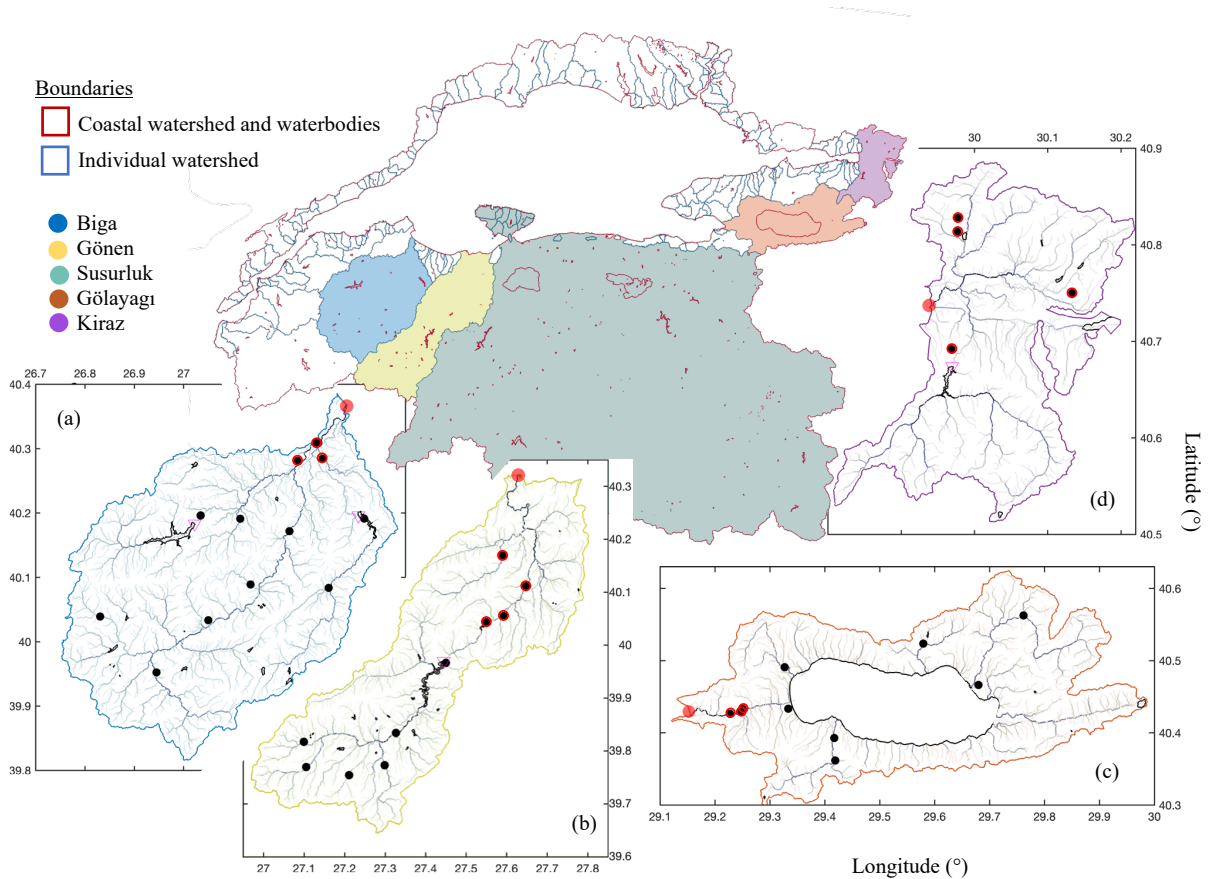


Figure 2. Coastal watershed of the Sea of Marmara with the study area shown in color. River network of the (a) Biga, (b) Gönen, (c) Gölayağı, and (d) Kiraz watersheds. Black dots, red dots, and pink triangles denote the water gages, river mouths, and dams, respectively; only the gages denoted by black dots with red circles are used in the analysis.

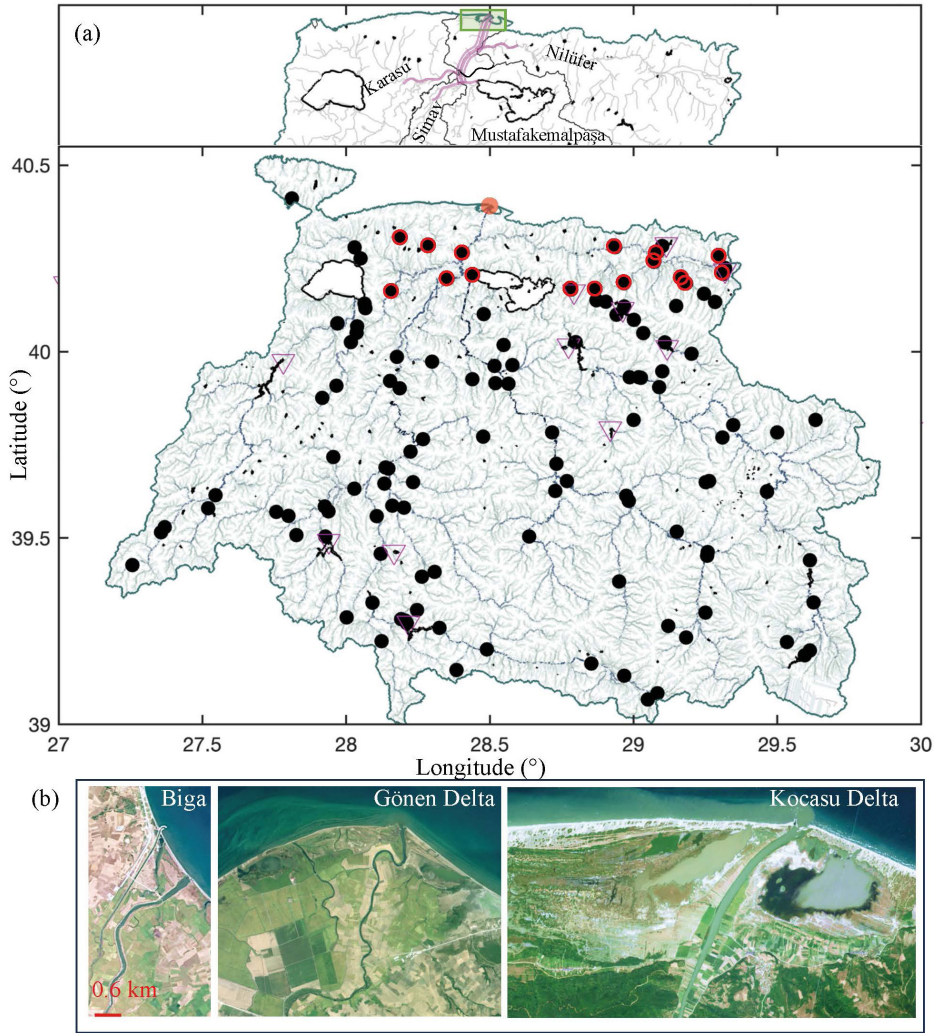


Figure 3. (a) Subbasins of the Susurluk (Çapraz River) watershed; tributaries from the subbasins are shown in pink (thin line) near the Çapraz River (thick line) junction. (b) Satellite images (<https://eos.com/landviewer>) of the river mouths of Biga, Gönen and Susurluk (Kocasu Delta).

alternative combinations of the stations closest to the river mouth, contributing to the coastal discharge (depicted as black markers with red circles), were chosen to estimate the daily discharge for the period 2010–2020. Because the operation dates of the gages differ, alternative station combinations were used for the period 1980–2020 to fill the gaps in the dataset. In addition, a nonparametric spectral estimation method (Yi and Sneeuw, 2021), which consists of single spectrum analysis, gap-filling techniques, cross-validation, and spectral testing, was used to fill temporal gaps. This approach allowed the utilization of trends in the data from the operational gages before 2010 to fill the relatively extensive gaps in the dataset for the period 2010–

2020. The operation periods and names of the gages used in this study are summarized in Table 1.

2.3. Daily precipitation and evaporation

Time series of cumulative daily precipitation and evaporation rates were obtained from the ERA5-Land database. The gridded datasets (9 km horizontal resolution) were spatially averaged for each watershed. The volume flux for each watershed was calculated by multiplying its drainage area with the spatial mean of cumulative daily discharge. Following this, the time series of both these volume fluxes and coastal discharges underwent low-pass filtering using a Savitzky-Golay filter with a 30-day window size to differentiate their daily variations.

Table 1. Names and operation periods of the streamflow gages used (i.e. black dots with red circles shown in Figures 3 and 4).

Names of the gauges		Operation period of the gauges used
Biga	E02A-001 -012 -014	1954–1958, 1961–1964 1965–1971, 1973–1989, 1991–2014, 2016–2020 1981–2008
Gönen	E02A-002 -007 -010 -015	1955–1958 1961–1971 1972–1994 1981–2004
Susurluk	D03A-023 -027 -029 -032 -033 -035 -064 -070 -071 -082 -092 -100 -115 -133 E03A-017 -021	1969–1982 1969–1988, 1996–2007, 2009–2020 2002–2004 1979–1983 1976–1978 1971–1975, 1979–1983 1984–2008, 2012–2020 1985–1990 1984–1986 K1986–1997, 2001–2020 1990–1996, 1999–2004 S1995–1997, 2002–2012 2004–2007, 2012–2020 2002–2020 M1953–1958, 1964–2020 1954–2006
Gölayağı	D02A-082 D03A-060 E02A-008	1984–1996 1983–1985 1965–1969
Kiraz	D02A-006 -061 -072 -078	1966–1971, 1976–1996, 1998–2020 1977–1981 1985–1988, 1990–1992 1982–1993

3. Results

3.1. Watersheds and stream network

Each studied watershed has a unique shape and corresponding river network (Figure 2). The bigger watersheds extend perpendicularly to the main river channel in the upstream direction, e.g., the Gönen and Susurluk watersheds. Consequently, these basins are more sensitive to floods due to their larger sediment transport capacities. The main channel of the Kiraz watershed splits into two tributaries, upsloping in opposite directions. Its northern tributary controls the daily extremes in river flow (controlled flow in the southern tributary, i.e. dam at the upstream of the southern gage). The presence of

lakes located near the coast on flatlands and connected to tributaries of the main channel modifies the coastal impact of extreme flood events. In the study area, the Gölayağı stream originates from Lake İznik, and the Çapraz River, the main channel of the Susurluk watershed (Figure 3a), has tributaries connected to the Manyas and Ulubat Lakes (Mustafakemalpaşa and Karasu rivers). These two tributaries, along with the Simav and Nilüfer rivers, merge onto the Çapraz River. There are agricultural fields and a wetland (the Kocasu delta with lagoons) on both sides of the main channel before it drains into the sea (Figure 3b, right panel). These features, combined with the geological ones (Figures A and 1), control the coastal discharge,

reducing its extreme flow rates during heavy precipitation. With flat alluvial river mouths, the agricultural fields of Gönen (Gönen Delta) and Biga (Figure 3b) have similar effects, the latter to a smaller extent.

3.2. Daily coastal discharge

The coastal discharge, estimated using the data from nearby gages, is shown in a clockwise direction from the Kiraz to the Biga River for each watershed, including the Nilüfer River, a tributary of the Çapraz River (Figure 4). For the period 2010–2020, the extreme discharges (thin line) observed in each watershed are 45, 18, 600, 250, and 350 $\text{m}^3 \text{s}^{-1}$ in the Kiraz, Gölayağı, Çapraz, Gönen, and Biga rivers, respectively; the monthly-mean peaks (thick line) are 20, 5, 300, 50, and 75 $\text{m}^3 \text{s}^{-1}$ on average.

The flow rates spatially differ along the coast in terms of their daily trends relative to the monthly averages, as well as in the intensity and frequency of extreme events. The rivers in the eastern watersheds show volume flux

extremes that are twice their monthly averages, while the daily extremes of the Gönen and Biga rivers increase up to four times their monthly averages. The Kiraz stream has the highest frequency of daily extremes, followed by the Biga and Gönen rivers. The flux of the Nilüfer stream, a tributary of the Çapraz River, shows a declining trend, contributing insignificantly and rarely to daily extremes in recent years, with a maximum contribution of up to 5 $\text{m}^3 \text{s}^{-1}$ to the Çapraz River outflow. The Çapraz River shows high monthly peaks rather than daily extremes due to its distinctive geomorphology and land use, with rare daily extremes (last significant one observed in early 2019).

The observations exhibit seasonal variation, with higher flow rates predominantly observed in the winter and early spring. The seasonal peaks of the monthly averaged flow rates vary spatially, with multiple yearly peaks (midwinter and midspring) in the Biga River, early winter and late spring in the Gönen River, and a single

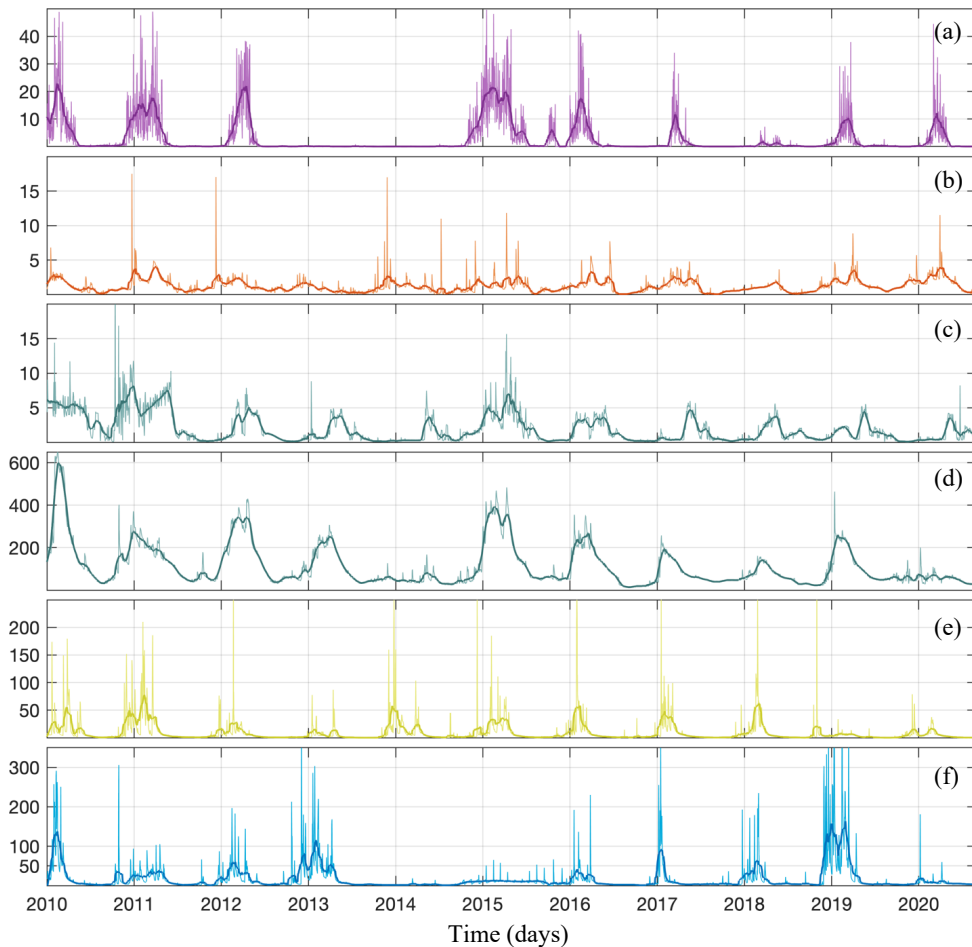


Figure 4. Daily coastal discharge rates of (a) Kiraz, (b) Gölayağı, (c) Nilüfer, (d) Çapraz, (e) Gönen, and (f) Biga streams associated with the watersheds shown in Figures 2 and 3. The thick line denotes the monthly change.

peak (late winter) in the Susurluk watershed. The Nilüfer River shows (gage located approximately 20 km inland from the coast) late spring peaks due to the melting snow from the higher altitudes. The summer flux peaks of the Gölayağı River are associated with the surface levels of the İznik Lake. The average seasonal volume fluxes of the watersheds are summarized in Table 2.

3.3. Precipitation and evaporation

The change in precipitation is shown as volume flux (Figures 5a–5e), with daily peaks of 200, 270, 4000, 700, and 700 $\text{m}^3 \text{s}^{-1}$ in the Kiraz, Gölayağı, Çapraz, Gönen, and Biga Rivers; the monthly-mean peaks (thick line) are approximately 50, 90, 1000, 200, and 200 $\text{m}^3 \text{s}^{-1}$. Precipitation extremes are primarily observed between late fall and early spring, but in recent years, extreme precipitation events have also occurred in the summer. The seasonal averages of precipitation rates decrease between May and mid-August, i.e. there is an order of magnitude drop in volume fluxes (Figure 5f). The increase in evaporation averages begins early in the spring and peaks in June (Figure 5g). The seasonal change

in coastal discharge mostly corresponds to the change in precipitation rates (Figure 5h). The response of the Çapraz River discharge to increasing precipitation and decreasing evaporation is slower compared to its response to decreasing precipitation and increasing evaporation. Despite their similar precipitation and evaporation trends, the discharges of the Biga and Gönen Rivers differ. The Gönen River has smaller flow rates, particularly during the summer months.

3.4. Anomalies of extreme events

The annual differences between daily and monthly variations in precipitation and coastal discharge are analyzed to determine the range of extreme event anomalies (Figure 6). The precipitation anomalies in the eastern basins vary from 100 $\text{m}^3 \text{s}^{-1}$ to 400 $\text{m}^3 \text{s}^{-1}$. Among the southern basins, the anomalies of the Susurluk watershed are the smallest, with a range similar to the eastern basins; larger ranges are found in the Biga and Gönen watersheds, varying from 100 $\text{m}^3 \text{s}^{-1}$ to 600 $\text{m}^3 \text{s}^{-1}$. Extreme events mostly occur in winter or fall; however, in the Biga, Gönen, and Kiraz watersheds, the peaks are observed in midsummer.

Table 2. Annual coastal discharge and total freshwater amount from the watersheds in the study area.

	Kiraz ($\text{m}^3 \text{s}^{-1}$)	Gölayağı ($\text{m}^3 \text{s}^{-1}$)	Susurluk ($\text{m}^3 \text{s}^{-1}$)	Gönen ($\text{m}^3 \text{s}^{-1}$)	Biga ($\text{m}^3 \text{s}^{-1}$)	Total	
						($\text{m}^3 \text{s}^{-1}$)	(kt)
January	4.7	1.6	160	18	41	225	585
February	7.9	1.7	225	27	48	310	806
March	8.9	2	219	21	31	282	733
April	6.3	2	177	12	18	215	559
May	1.8	1.5	125	5	8	141	366
June	0.7	1.2	89	2	5	98	254
July	0.2	0.6	57	1	4	63	163
August	0.1	0.3	39	1	4	44	114
September	0.2	0.5	42	1	4	48	124
October	0.6	0.6	54	2	7	64	166
November	0.8	1.1	60	6	9	77	200
December	1.9	1.6	80	14	25	123	319
Total	34	15	1327	110	204	1690 ($\text{m}^3 \text{s}^{-1}$)	
	88	39	3450	286	530	4394 (kt)	

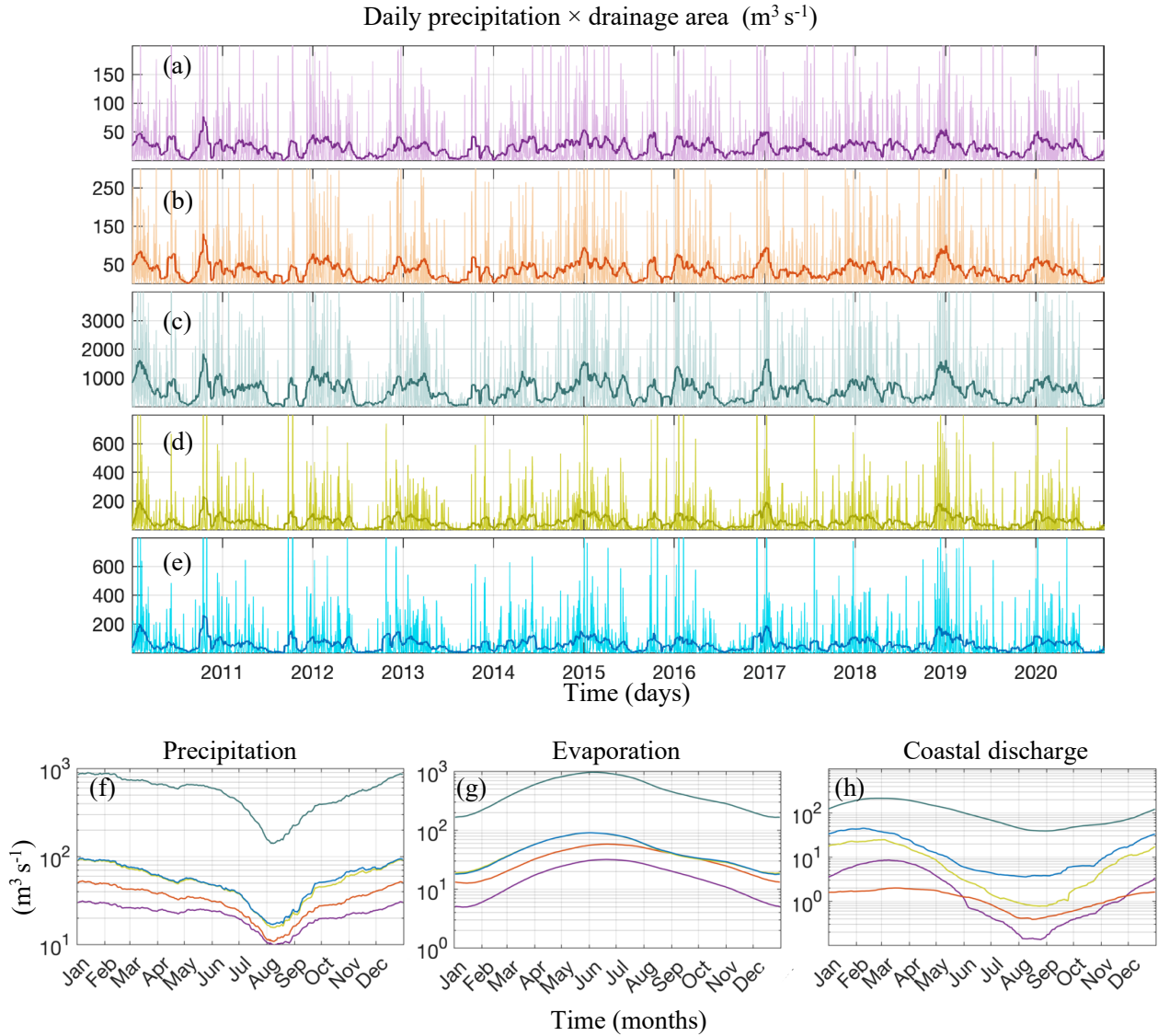


Figure 5. Daily cumulative precipitation times the watershed area for the basins associated with the (a) Kiraz, (b) Gölayağı, (c) Çapraz, (d) Gönen, and (e) Biga streams with the thick line denoting the monthly change. Yearly averaged precipitation and evaporation times the watershed area (f and g), and (h) yearly averaged coastal discharge.

The discharge anomalies are smallest in the eastern basins ($10\text{--}30 \text{ m}^3 \text{ s}^{-1}$), and an order of magnitude greater in the southern basins (up to $400 \text{ m}^3 \text{ s}^{-1}$), with the biggest ranges observed in the Biga watershed. The results suggest that the monthly change in discharge from the Çapraz River is more significant than the daily extremes. When compared to the precipitation anomalies, the coastal discharge extremes are more sensitive to the precipitation anomalies in fall, winter, and early spring, except for the Gölayağı stream. The discharge response of the Gölayağı stream differs due to the change in water levels in the İznik Lake.

4. Discussion

The main finding of this study is the quantification of the daily coastal discharges in the prominent watersheds of the Sea of Marmara and their potential impact on the health of marine waters. The results suggest that extreme coastal discharges combined with increasing concentrations of pollutants pose a threat to the ecosystem.

The coastal discharge shows seasonality with an annual change in net precipitation rates. The extreme river discharges mostly follow the extreme precipitation events, peaking between late fall and early spring. During summer, the anomalies in precipitation extremes and their impact

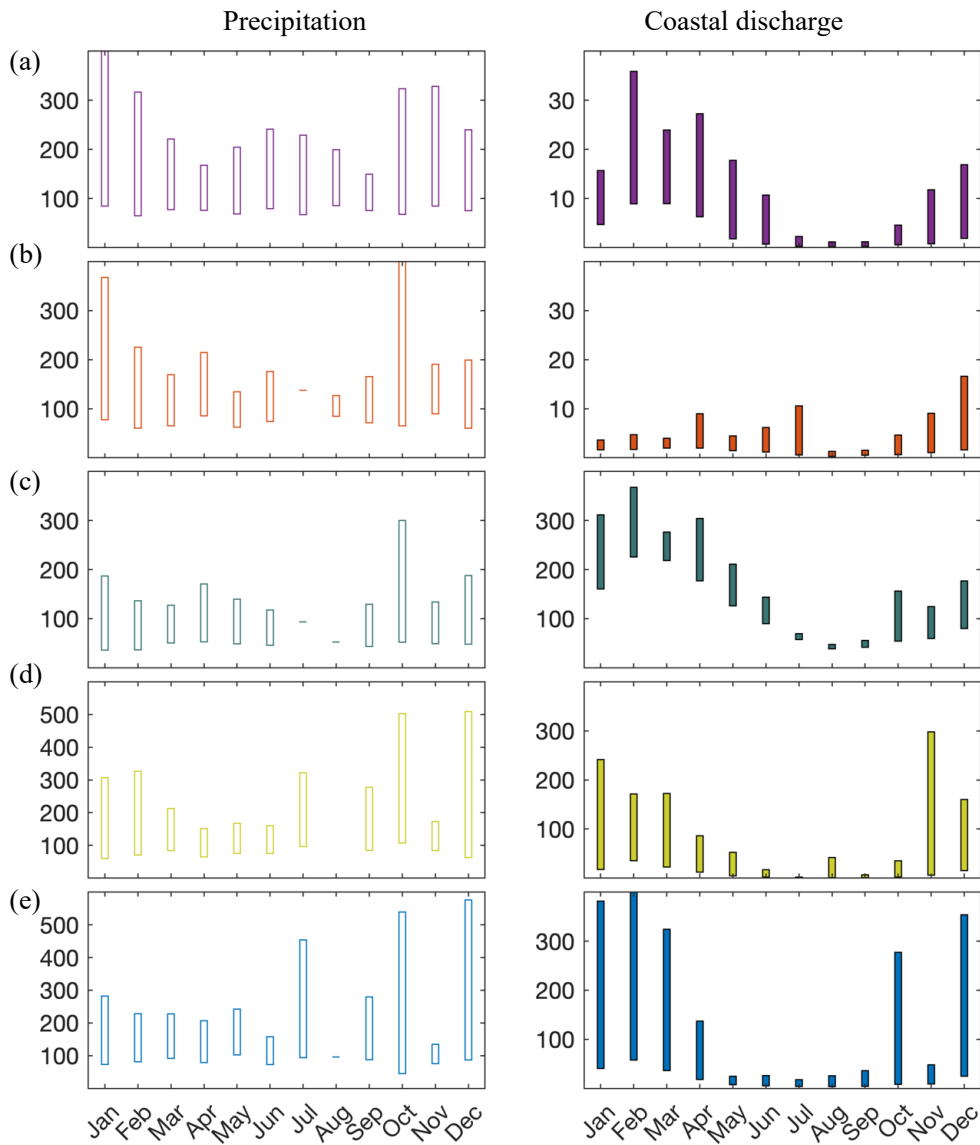
Extreme event anomalies ($\text{m}^3 \text{s}^{-1}$)

Figure 6. Seasonal anomalies of the daily precipitation extremes (left panel) and the coastal discharge extremes (right panel) for each watershed (rows): (a) Kiraz, (b) Gölayağı, (c) Çapraz, (d) Gönen, and (e) Biga streams.

on discharge rates are compensated by high evaporation rates. Additionally, the geomorphology, shape, land use, vegetation of watersheds and riverbanks, and the presence of lakes affect the relationship between atmospheric input and coastal discharge peaks. The meandering shape of the Gönen River and its triangular delta dampen the extreme upstream discharges. The coastal zone of the Biga River is more sensitive to instantaneous flow peaks, whereas the coast of the Susurluk watershed is prone to monthly peaks rather than daily extremes.

During flood events, excess water overflowing from the riverbanks is retained in agricultural fields and wetlands (southern watersheds). Therefore, these extremes do not reach the river mouth. This is due to the land use and geomorphology of the southern watersheds (alluvial flatlands with agricultural fields). Owing to the absence of gages at the river mouth, the thresholds for discharge peaks in these basins were estimated based on the channel shape, the structure of the land between the coastline and the gage location, and satellite images of river plumes

after heavy precipitation (determined by competitively analyzing the surface area of the southern river outflows; not shown).

The thresholds for extreme daily discharges are estimated as 175, 100, and 300 m³ s⁻¹ for the Biga, Gönen, and Çapraz Rivers; the volume flux greater than the threshold value spreads over the land; part of it is retained and infiltrates into the sedimentary basin (seepage), while another portion moves to the coast through a slow surface runoff.

From an environmental perspective, instantaneous nutrient loads with high flow rates may trigger extreme events due to an abrupt change in the nutrient balance of the system.

With decreasing nutrient loads from the Black Sea (Polat and Tuğrul, 1995; Oguz, 2017; Cozzi et al., 2018), terrestrial nutrient loads (increasing concentrations with intense discharges) have the potential to create conditions for extreme events, such as sea snout. The underlying mechanism that triggers such conditions may be related to excessive nitrate input that changes the nutrient ratio, leading to the accumulation of organic matter in the intermediate layers. These events have a long-lasting impact, particularly in the bays of Erdek, Bandırma, and gulfs of Gemlik and İzmit, where flow circulation is relatively weak. Tan (2021) found the pressure exerted by land-based sources on Bandırma Bay and gulfs of İzmit and (Inner) Gemlik to be high, and on Erdek Bay and Gulf of (Outer) Gemlik to be moderate based on the Pressure Index method.

In the eutrophication assessment of coastal waters, the national regulations differ in the parameters used and the upper limits associated with these parameters (Tan, 2021). Therefore, collecting these regulations under a single heading and updating them is important to accurately monitor and assess water quality of the coastal waters of the Sea of Marmara. The implementation of measures proposed for the coastal watersheds by TÜBİTAK MAM (2010), ÇŞB ÇEDİDGM and TÜBİTAK-MAM (2020), ÇŞİDB and ODTÜ-DBE (2021) is crucial. Among these measures, the treatment and monitoring of urban and industrial wastewater, whether carried (point or surface) directly or indirectly (via rivers) into the sea, the quantification and limitation of nutrient loads carried via agricultural wastes, and the restoration of the riverbanks are of primary importance.

Climate change adversely affects coastal and transitional ecosystems with rising temperatures and sea levels, more erratic rainfall, and freshwater discharges, resulting in more frequent or more severe droughts and storms (Day and Rybczyk, 2019). In the watersheds of the Sea of Marmara, the extreme precipitation events pose a threat to the region, increasing the risk of flood events (Basdurak, 2023). Moreover, elevated rates of relative sea level rise can also accelerate vegetation changes in coastal wetlands (He and Silliman, 2019). The Kocasu and Gönen deltas are prone to such changes. Thus, investing in local conservation, such as the restoration of the deltas and wetlands and increasing vegetation around the riverbanks and wetlands, plays a significant role in dampening the adverse effects of such extreme events and enhancing the resilience of the coastal zone.

Because the watersheds have unique characteristics that affect the timing and intensity of coastal discharges, individual monitoring of nutrient concentrations and pollutants in the watersheds near the coast is necessary. This way, the coastal fluxes of nutrients and pollutants from riverine sources can be accurately identified. Most importantly, both the formation or propagation of extreme events, such as sea snout, can be prevented by early recognition, and measures can be taken to decelerate the deoxygenation of the Sea of Marmara.

The daily changes in coastal discharges provided in this study can be used in ocean models focusing on small-scale processes and biogeochemical dynamics. Additionally, the dataset can be adopted in catchment models to predict nutrient dynamics. However, when using the dataset, it is recommended to employ thresholds for extreme discharge values in the southern watersheds.

Acknowledgment

I gratefully thank Prof. Dr. Süleyman Tuğrul for our valuable discussions. I also express my thanks to the Ministry of Environment, Climate Change and Urbanization of Türkiye and the General Directorate of State Hydraulic Works for their assistance in providing the historical streamflow dataset in a standardized format in conjunction with “The Marmara Integrated Modelling System Project (MARMOD) - Phase II (2021.09.00.2.00.002)” and METU-IMS-DEKOSIM (2012-K-120880).

References

- Algan O (2006). Riverine fluxes into the Black and Sea of Marmara. In Fluxes of Small and Medium-size Mediterranean Rivers: Impact on Coastal Areas. The Mediterranean Science Commission Workshop Monographs 30: 47-53.
- Başdurak BN. (2023) Climate change impacts on river discharge to the Sea of Marmara. *Frontiers in Marine Science* 10: 1278136. <https://doi.org/10.3389/fmars.2023.1278136>
- Beşiktepe S, Sur Hİ, Özsoy E, Latif MA, Oğuz T et al. (1994). Circulation and hydrography of the Marmara Sea. *Progress in Oceanography* 34: 285-334. [https://doi.org/10.1016/0079-6611\(94\)90018-3](https://doi.org/10.1016/0079-6611(94)90018-3)
- Cozzi S, Ibáñez C, Lazar L, Raimbault P, Giani M (2018). Flow regime and nutrient-loading trends from the largest South European watersheds: Implications for the productivity of Mediterranean and Black Sea's Coastal Areas. *Water* 11 (1): 1. <https://doi.org/10.3390/w11010001>
- Çevre, Şehircilik ve İklim Değişikliği Bakanlığı, TÜBİTAK Marmara Araştırma Merkezi (2020). Denizlerde Bütünlük Kirlilik İzleme İşi 2017-2019, Marmara Denizi Özet Raporu (TÜBİTAK Marmara Araştırma Merkezi Matbaası Gebze/Kocaeli/Ankara, Türkiye) (in Turkish).
- Çevre, Şehircilik ve İklim Değişikliği Bakanlığı, Orta Doğu Teknik Üniversitesi Deniz Bilimleri Enstitüsü (2021). Marmara Denizi Bütünlük Modelleme Sistemi FAZ II Projesi (MARMOD - FAZ II) 2021 Yılı Ara Raporu (Ankara, Türkiye) (in Turkish).
- Day JW, Rybczyk JM (2019). Global change impacts on the future of coastal systems: perverse interactions among climate change, ecosystem degradation, energy scarcity, and population. *Coasts and Estuaries* (pp. 621-639). Elsevier. <https://doi.org/10.1016/B978-0-12-814003-1.00036-8>
- Ediger D, Beken Ç, Yüksek A, Tuğrul S. (2016). Eutrophication in the Sea of Marmara. *The Sea of Marmara - Marine Biodiversity, Fisheries, Conservation and Governance*, Turkish Marine Research Foundation Press, İstanbul (2016), pp. 723-736.
- Elliott M, Day JW, Ramachandran R, Wolanski E (2019). A synthesis: what is the future for coasts, estuaries, deltas and other transitional habitats in 2050 and beyond? In *Coasts and estuaries* (pp. 1-28). Elsevier. <https://doi.org/10.1016/B978-0-12-814003-1.00001-0>
- He Q, Silliman BR (2019). Climate change, human impacts, and coastal ecosystems in the Anthropocene. *Current Biology*, 29 (19): pp. R1021-R1035. <https://doi.org/10.1016/j.cub.2019.08.042>
- Latif MA, Tezcan D, Yücel M, Örek H, Tuğrul S et al. (2022). Marmara Denizi 2015-2021 yılları arası yüzey sıcaklık ve tuzluluk değişimleri. Marmara Denizi 2022 Sempozyumu Bildiriler Kitabı. Türk Deniz Araştırmaları Vakfı, Yayın no: 63, İstanbul, Türkiye (in Turkish).
- Oğuz T (2017). Controls of multiple stressors on the Black Sea fishery. *Frontiers in Marine Science* 4: 110. <https://doi.org/10.3389/fmars.2017.00110>
- Ozbayram EG, Akcaalan R, Isinibilir M, Albay M (2022). Insights into the bacterial community structure of marine mucilage by metabarcoding. *Environmental Science and Pollution Research* 29 (35): 53249-53258. <https://doi.org/10.1007/s11356-022-19626-9>
- Polat SÇ, Tuğrul S (1995). Nutrient and organic carbon exchanges between the Black and Marmara Seas through the Bosphorus Strait. *Continental Shelf Research* 15 (9): 1115-1132. [https://doi.org/10.1016/0278-4343\(94\)00064-T](https://doi.org/10.1016/0278-4343(94)00064-T)
- Savun Hekimoğlu B, Gazioğlu C (2021). Mucilage problem in the semi-enclosed seas: Recent outbreak in the Sea of Marmara. *International Journal of Environment and Geoinformatics*, 8 (4): 402-413. <https://doi.org/10.30897/ijegeo.955739>
- Tan İ (2021). Marmara denizi körfezlerinin baskı - etki durumu ve ötrofikasyon açısından değerlendirilmesi. *Aquatic Research*, 4 (2): 169-180 (in Turkish). <https://doi.org/10.3153/AR21014>
- Tavsanoğlu UN, Akbulut NE (2019). Seasonal dynamics of riverine zooplankton functional groups in Turkey: Kocaçay Delta as a case study. *Turkish Journal of Fisheries and Aquatic Sciences* 20 (1): 69-77. https://doi.org/10.4194/1303-2712-v20_1_07
- Tuğrul S, Beşiktepe T, Salihoğlu I (2002). Nutrient exchange fluxes between the Aegean and Black Seas through the Sea of Marmara. *Mediterranean Marine Science*, 3 (1): 33- 42. <https://doi.org/10.12681/mms.256>
- Tuğrul S, Gürses O, Yüksek A (2015). MAREX: Turkish Straits System - Marmara Sea Experiments report, Middle East Technical University, Institute of Marine Science, pp 33.
- TÜBİTAK Marmara Araştırma Merkezi (2010). Havza Koruma Eylem Planlarının Hazırlanması projesi-Marmara Havzası. Proje Nihai Raporu, TÜBİTAK Marmara Araştırma Merkezi Matbaası Gebze Kocaeli. (Proje Sahibi Kurum: Çevre ve Orman Bakanlığı). S466 (in Turkish).
- Ünlüata Ü, Oğuz T, Latif MA, Özsoy E (1990). On the Physical Oceanography of the Turkish Straits, in: *The Physical Oceanography of Sea Straits*, L. J. Pratt (editor), NATO/ASI Series, Kluwer, Dordrecht, 25-60. https://doi.org/10.1007/978-94-009-0677-8_2
- Yıldız D, Güneş MS, Gökalp YE, Yıldız D (2018). Detecting seasonal cycle shift on streamflow over Turkey by using multivariate statistical methods. *Theoretical and Applied Climatology*, 133: 1143-1161. <https://doi.org/10.1007/s00704-017-2242-2>
- Yücel M, Özkan K, Fach B, Tuğrul S (2021). Marmara Denizi'nin Ekolojisi: Deniz Salyası Olusumu, Etkileşimleri ve Çözüm Önerileri (Ankara: Turkish Academy of Sciences).

Appendix A: Geological features of the watersheds

The geological map of the coastal watersheds in the study area (Figure A) is adopted from the 1:500,000 scaled quadrangle for İstanbul (MTA, 2021). The map shows distinct geological features in the eastern and southern watersheds that contribute to the variability in the net precipitation flow rate relations. These geological features and their changes around the river tributaries in the downstream direction near the river mouth can potentially alter the coastal discharge during heavy rainfall and floods.

²Maden Tetkik ve Arama (2021). Geological map of Türkiye, 1:500,000 scale İstanbul quadrangle. Geological Research Department, General Directorate of Mineral Research and Exploration, Ankara, Türkiye [online]. Website: <https://www.mta.gov.tr/v3.0/sayfalar/hizmetler/doc/ISTANBUL.pdf> [accessed 2023/05/30]

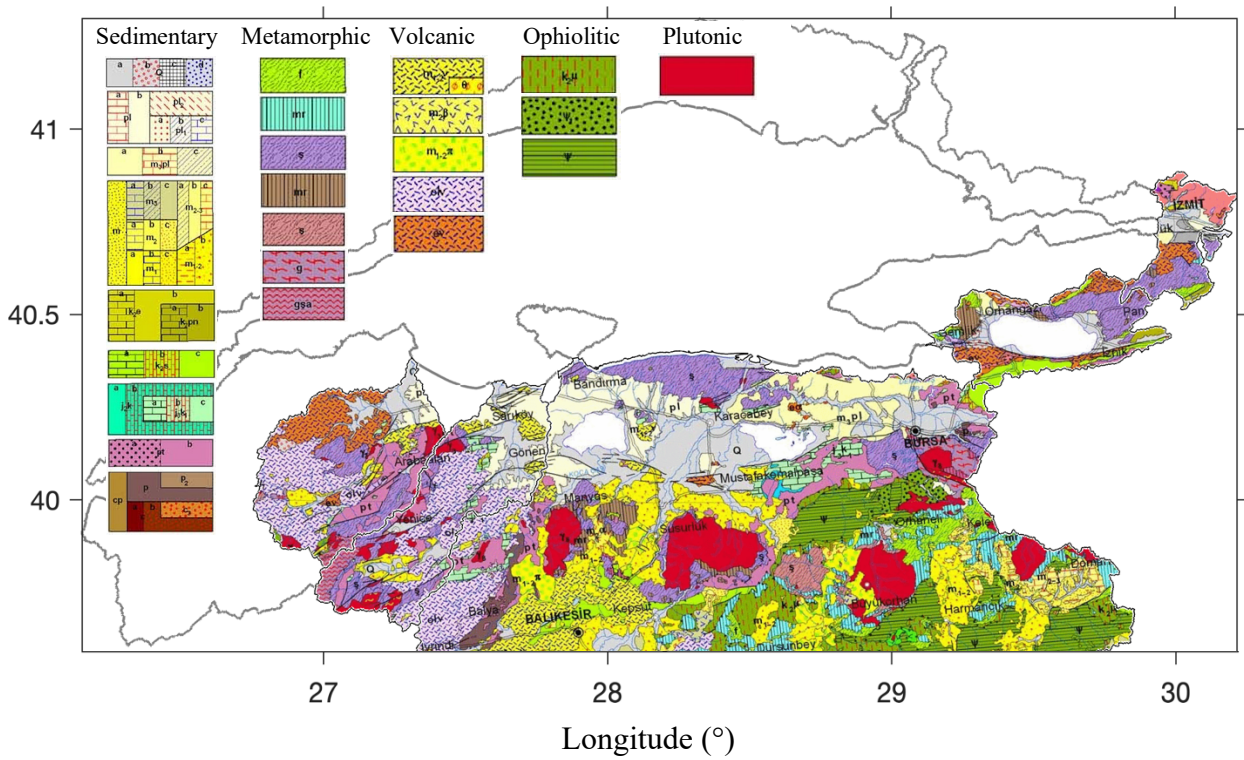


Figure A. Geological map of the study area, adopted from MTA (2021).